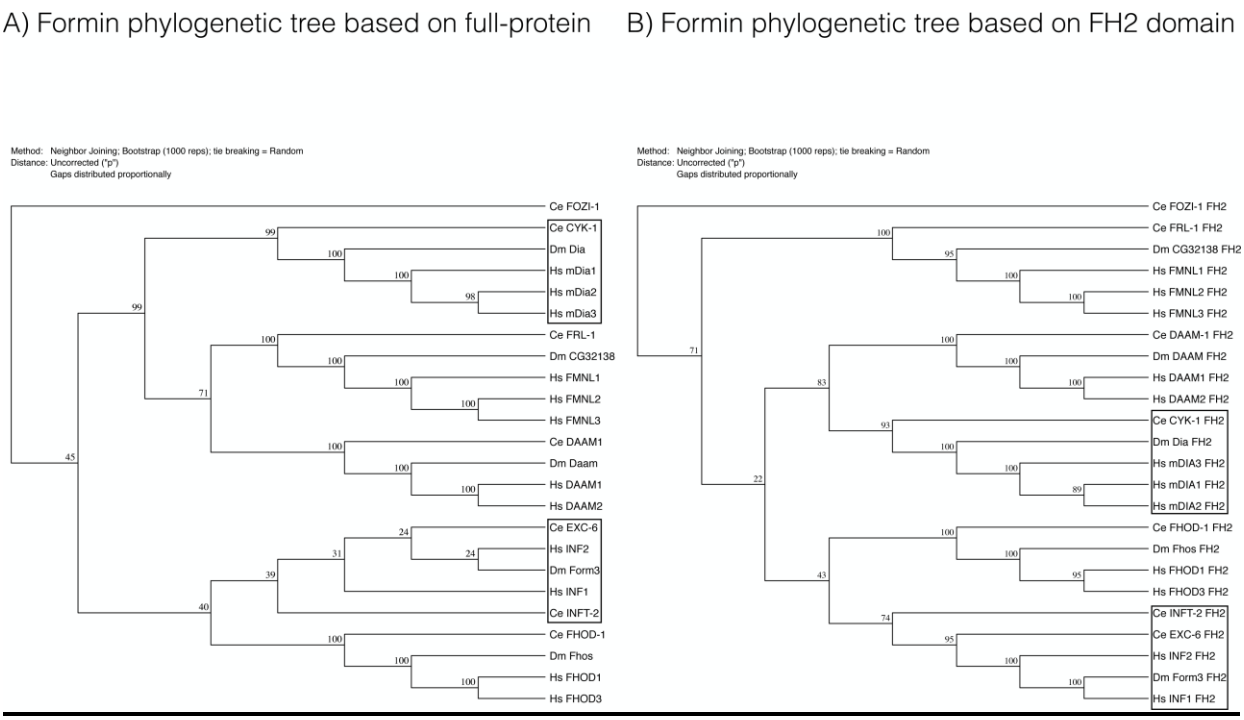

Fig. S1. Phylogenetic analyses of *C. elegans* (Ce), *Drosophila* (Dm) and human (Hs) formins. We generated phylogenetic trees using **(A)** the full-length sequences or **(B)** the FH2 domain alone, as had been previously done (Chalkia et al., 2008; Liu et al., 2010; Mi-Mi et al., 2012). In both panels, the mDia and INF2 families are highlighted. Protein sequences were aligned using the ClustalW function of MacVector (MacVector, Inc. Apex, NC. USA), using the Gonnet matrix with default settings. Phylogenetic trees were generated in MacVector using the neighbor joining method with 1000 bootstrap repetitions. Percent branch support is shown for all branches. We rooted the trees with Ce FOZI-1, a highly divergent formin-like nuclear protein that influences cell fate choices but does not interact with actin (Johnston et al., 2006). We note that for the INF2 family, using full-length sequences provides low bootstrap support for branching, likely due to divergence in sequences outside the catalytic FH1/FH2 domains. However, both *C. elegans* INF2 paralogs clearly cluster within this family, and using the FH2 domain alone to elucidate relationships between INF2 family members provides more reliable clustering.

Mutated in FSGS (Brown, et al., 2010; Boyer et al., 2011a). Shaded (E184 and R218) are required in INF2-DID for interaction with mDia-DAD (Sun, et. al., 2011).

Mutated in FSGS + CMT (Boyer, et al., 2011b).

Mediate intramolecular DID-DAD interaction in mouse mDia1 (Nezami, et al., 2006).

Fig. S2. Residues required for intra- and inter-molecular DID/DAD interactions, and residues mutated in human disease, are conserved in the divergent INFT-2 "DID". Alignment of the DID regions of human (Hs) INF2 and *C. elegans* (Ce) INFT-2. We used the mouse (Mm) mDia1 DID sequence as a reference, because it has been crystallized bound to its DAD and used to define DID/DAD interacting residues (Nezami et al., 2006). These residues are highlighted in blue here. We note that many of these are conserved in the divergent INFT-2 DID, including some that when mutated affect mDia DID/DAD interactions (e.g. mDia1 Ile222, corresponding to INFT-2 Ile214, mDia1 Ile259, corresponding to INFT-2 Val258, and mDia1 Leu260, corresponding to INFT-2 Leu 259). Residues mutated in INF2 that lead to FSGS or FSGS+CMT are highlighted in Green and Red, respectively. The two residues tested that affected INF2-DID to mDia-DAD interaction (Sun et al., 2011), Glu184 and Arg218, are conserved in Ce INFT-2 (shaded).

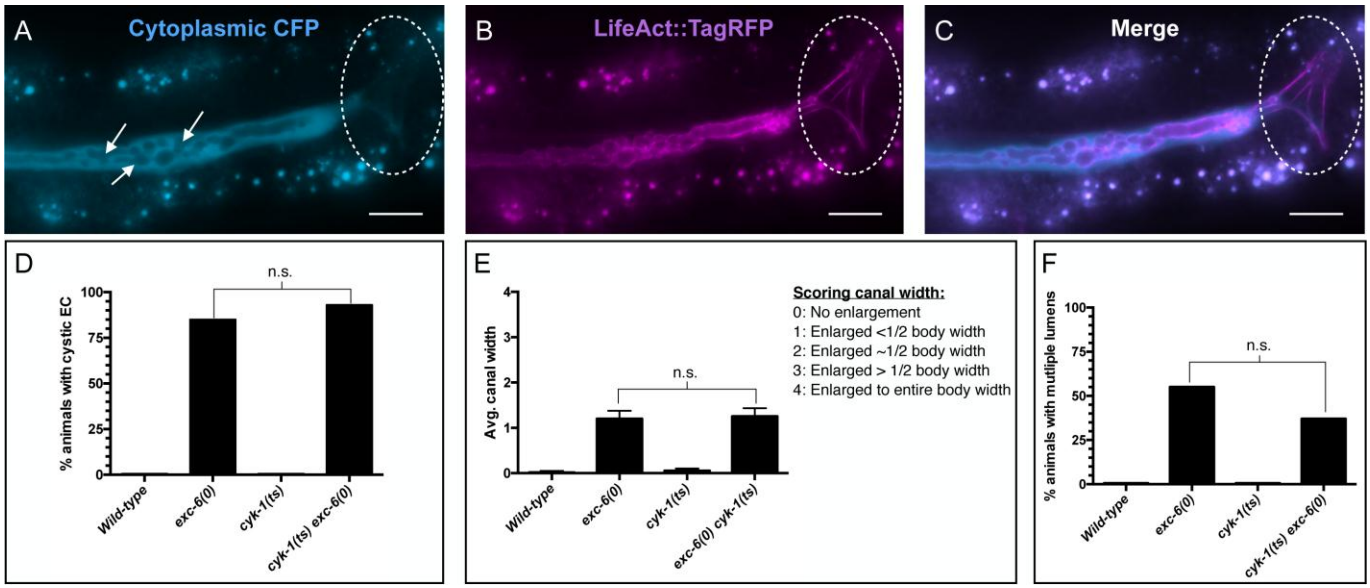

Fig. S3. Phenotypes in *cyk-1(ts) exc-6(0)* double mutants resemble those seen in *exc-6(0)* alone. Photomicrographs **(A-C)** showing multiple lumens (arrows) and a disorganized F-actin structure at the leading edge (dashed circle), both characteristic phenotypes of *exc-6(0)* mutants (Shaye and Greenwald, 2015). Images were acquired via wide-field microscopy, using a Plan-Apochromat 40x/1.4 Oil objective, as described in Materials and Methods. Scale bar is 10µm. Quantification of the **(E)** penetrance and **(F)** severity of the cystic phenotype, as well as the **(G)** penetrance of the multiple lumen phenotype in *wild-type* (n=30), *exc-6(0)* (n=60), *cyk-1(ts)* (n=60) and *cyk-1(ts) exc-6(0)* doubles (n=43). Significance for penetrance of cystic and multiple lumen phenotypes was calculated by a two-tailed Fisher's exact test. Significance for the severity of the cystic phenotype was calculated with a Mann-Whitney test.

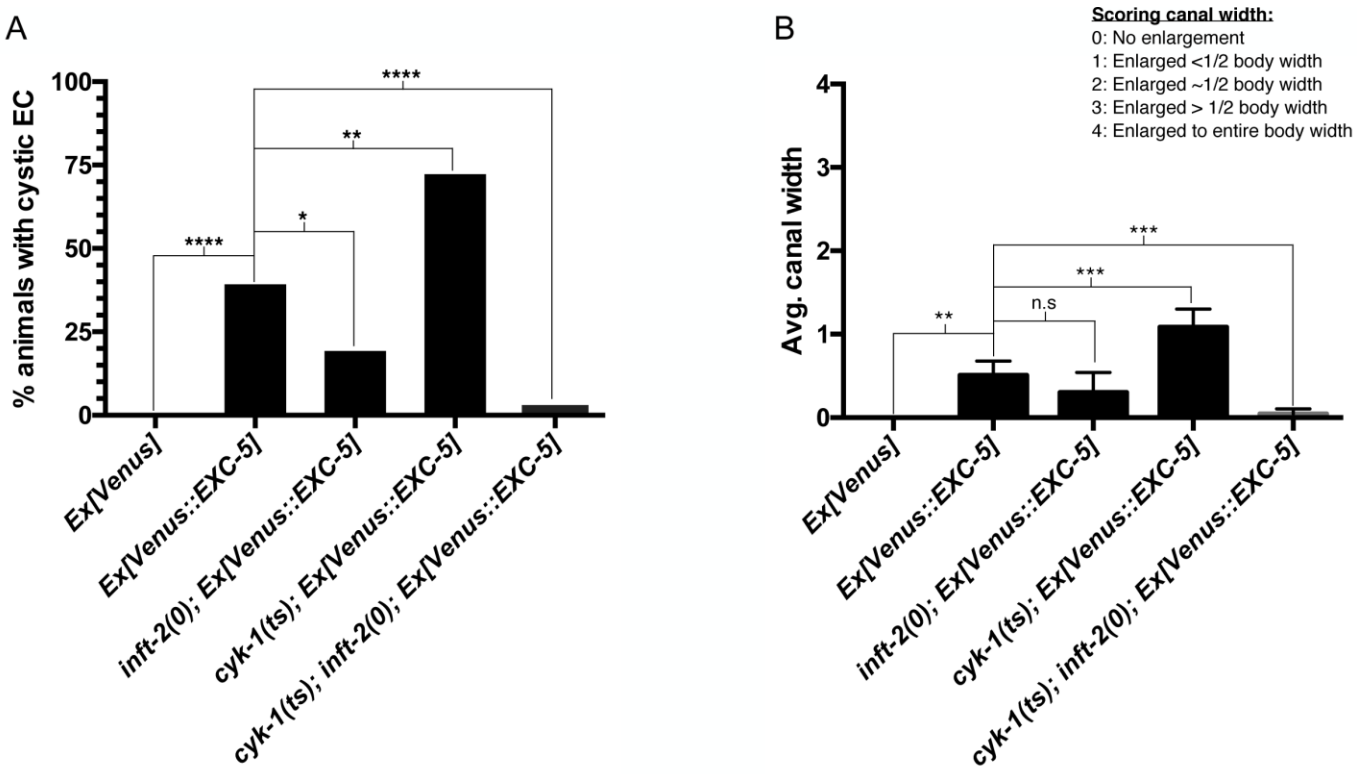

Fig. S4. Other phenotypes caused by Venus::EXC-5 overexpression are also modified by *inft-2(0)* and *cyk-1(ts)*. Quantification of the **(A)** penetrance and **(B)** severity of the cystic phenotype in *wild-type* carrying *arEx2404* (*Ex[Venus]* n=30), *wild-type* carrying *arEx2360* (*Ex[Venus::EXC-5]* n=65), *inft-2(0); arEx2360* (n=30), *cyk-1(ts); arEx2360* (n=60) and *cyk-1(ts); inft-2(0); arEx2360* (n=46). Significance for penetrance the cystic phenotype was calculated by a two-tailed Fisher's exact test. Significance for the severity of the cystic phenotype was calculated with a Kruskal-Wallis test for multiple comparisons.

Movie 1. Venus::CYK-1 (yellow) is cytoplasmic and is also found in dynamic juxta-apical punctae in *wild-type*. Arrows mark the first appearance of punctae that were visible for at least two frames (~90 seconds). In this ~10-minute movie we counted at least 12 such punctae. F-actin, labelled with LifeAct::TagRFP (magenta), is found at the lumen-lining apical membrane, and can be seen accumulating in some of the juxta-apical Venus::CYK-1 labelled punctae. This movie is a maximum projection of seventeen 1µm z-steps taken using the settings for Venus::CYK-1 described in the "Spinning Disk Microscopy Settings" section of the Supplementary Materials and Methods.

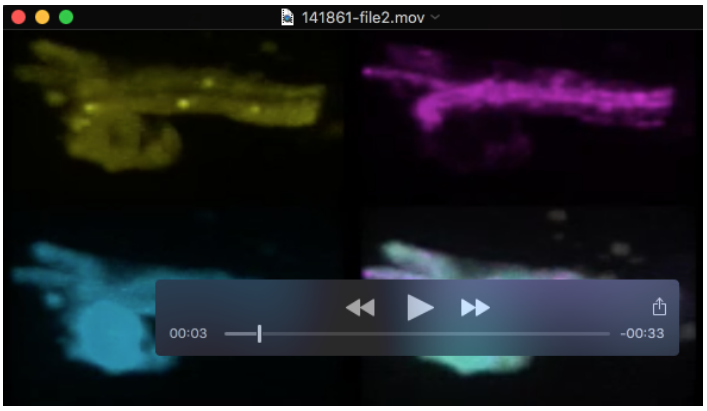

Movie 2. 3D projection of the same *wild-type* EC seen in Fig. 2F, showing that that when not present in juxta-apical punctae, Venus::CYK-1 appears cytoplasmic and reaches the basolateral side (entire cytoplasm is marked by CFP). Eight 1.0µm thick sections were used to generate this projection, and images were acquired as described for Venus::CYK-1 in the "Spinning Disk Microscopy Settings" section of the Supplementary Materials and Methods.

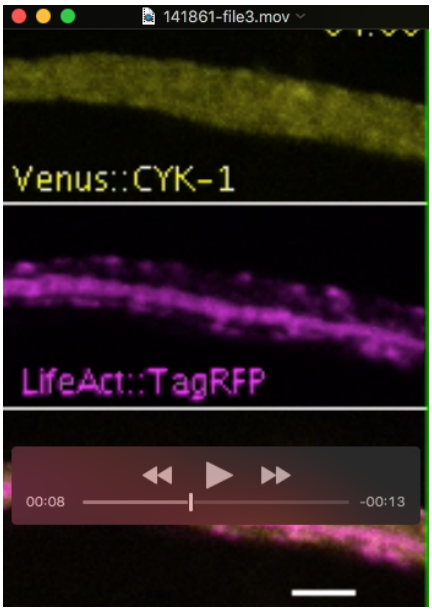

Movie 3. Venus::CYK-1 (yellow) accumulation in juxta-apical punctae is greatly reduced in *cdc-42(0*)*. Arrows mark the first appearance of punctae that were visible for at least two frames (~60 seconds). In this ~10-minute movie we only found 2 such punctae, and both were found near the basolateral domain, not juxta-apical (compare to *wild-type* Movie S1). F-actin, labelled with LifeAct::TagRFP (magenta), is found at the lumen-lining apical membrane and can be seen accumulating in some motile punctae, although most are not marked with Venus::CYK-1 and their localization is more variable than in *wild-type*. This movie is a maximum projection of four 1µm z-steps taken using the settings for Venus::CYK-1 described in the "Spinning Disk Microscopy Settings" section of the Supplementary Materials and Methods.

Supplementary Materials and Methods

Strains

Standard methods were used for strain handling and maintenance (Brenner, 1974). Mutant alleles are described in WormBase (www.wormbase.org). Primers used to confirm genotypes by sequencing or PCR are listed in the "Primers" table below. The following GFP-marked balancer chromosomes were used in crosses and to maintain sterile or lethal mutants: *mIn1[mIs14]*, *hT2[qIs48]*, *nT1[qIs51]* (Edgley et al., 2006), and *qC1[nIs189]* (Andersen et al., 2008).

Table S1. Strains

Strain	Genotype*	Figure(s)
GS6602	*arIs198*	1A, G. 3A, B. 4A, B
GS7284	*exc-6(gk386); arIs198*	1B, G. 3A
GS7022	*exc-5(rh232); arIs198*	1C, G. 4A, B
GS7266	*exc-6(gk386); exc-5(rh232); arIs198*	1D, G
GS8109	*cdc-42(gk388)/mIn1[mIs14]; arIs198*	1E, G
GS8110	*cdc-42(gk388)/mIn1[mIs14]; exc-6(gk386); arIs198*	1F, G
GS8124	*arIs195; arEx2360*	1H, J
GS8125	*cdc-42(gk388)/mIn1[mIs14]; arIs195; arEx2360*	1I, J
GS8122	*arIs195; arEx2411*	1J
GS7924	*arIs195; arEx2348*	2B
GS8115	*arIs198; arEx2406*	2C
GS8126	*cdc-42(gk388)/mIn1[mIs14]*; *arIs198; arEx2406*	2C
GS7933	*arIs195; arEx2357*	2D
GS8119	*arIs198; arEx2410*	2E
GS8127	*cdc-42(gk388)/mIn1[mIs14]*; *arIs198; arEx2410*	2E
GS6716	*inft-2(ok1296); arIs198*	3A. 4A, B
GS7637	*cyk-1(or596ts); arIs198*	3A. 4A, B
GS7025	*exc-6(gk386); inft-2(ok1296); arIs198*	3A
GS7638	*cyk-1(or596ts) exc-6(gk386); arIs198*	3A
GS7959	*cyk-1(or596ts); inft-2(ok1296); arIs198*	3A, C. 4A, B
GS7960	*cyk-1(or596ts) exc-6(gk386); inft-2(ok1296); arIs198*	3A
GS8113	*arIs198; arEx2404*	3D, 3E
GS8150	*cyk-1(or596ts); inft-2(ok1296); arIs198; arEx2404*	3D
GS8151	*cyk-1(or596ts); inft-2(ok1296); arIs198; arEx2406*	3D, 4C, D
GS8152	*cyk-1(or596ts); inft-2(ok1296); arIs198; arEx2410*	3D
GS7953	*arIs198; arEx2360*	3E
GS8120	*inft-2(ok1296); arIs198; arEx2360*	3E
GS8146	*cyk-1(or596ts); arIs198; arEx2360*	3E
GS8147	*cyk-1(or596ts); inft-2(ok1296); arIs198; arEx2360*	3E
GS8105	*cyk-1(ok2300)/qC1[nIs189]; arIs198*	Not shown
GS8106	*exc-6(gk386) cyk-1(ok2300)/exc-6(gk386) qC1[nIs189]; arIs198*	Not shown
GS8107	*cyk-1(ok2300)/qC1[nIs189]; inft-2(ok1296); arIs198*	Not shown

***:** Integrated *arIs* transgenes rescue *unc-119(ed3)*, and extrachromosomal *arEx* transgenes rescue *pha-1(e2123ts)*. These mutations may be present in some backgrounds for transgene selection. Full genotypes available on request.

Transgenes and Plasmids

Details of plasmid constructions are available upon request. Extrachromosomal transgenes were generated by germline micro-injection of plasmid mixes (Evans, 2006). Injection mixes contained the selection marker pBX, which rescues *pha-1(e2123ts)* (Granato et al., 1994), and the Hygromycin resistance construct pIR98 (Radman et al., 2013), both at 50ng/µl. Mixes with GFP-expressing fosmids were injected into *unc-119(ed3) pha-1(e2123ts); arIs195* hermaphrodites. Mixes with Venus-expressing constructs were injected into *unc-119(ed3) pha-1(e2123ts); arIs198* hermaphrodites. Transformants were selected by *pha-1(ts)* rescue at 25°C. Thereafter transgenes were followed by fluorescent expression of constructs, *pha-1(ts)* rescue, and/or survival on hygromycin plates.

Table S2. Transgenes and plasmids

Transgene	Construct(s)	Plasmid	Concentration
arIs195	*glt-3p::LifeAct::TagRFP*	See Shaye and Greenwald, 2015	
arIs198	*glt-3*p::*CFP*		
	*glt-3*p::*LifeAct::TagRFP*		
arEx2348	*inft-2::gfp*	fosmid	25 ng/µl
arEx2349			
arEx2357	*cyk-1::gfp* fosmid	fosmid	25 ng/µl
arEx2358			
arEx2360	*glt-3*p::*Venus::exc-5*	pDS630	6 ng/µl
arEx2361			
arEx2404	*glt-3*p::*Venus*	pDS242	6 ng/µl
arEx2411			
arEx2405	*glt-3*p::*Venus::inft-2*	pDS453	6 ng/µl
arEx2406			
arEx2408	*glt-3*p::*Venus::cyk-1b*	pDS631	6 ng/µl
arEx2409			
arEx2410			

Note: all *glt-3*p-driven constructs use the *unc-54 3'UTR*.

Primers

For primers used to amplify cDNAs, blue sequences are heterologous, restriction sites used for cloning cDNAs into pDS242, the *glt-3*p::*Venus::unc-54*'3 vector, are underlined, start and stop codons are bold.

Table S3. Primers

Oligo	Sequence	Use
oDS320	ATGGATTTACCAGCGCAAAG	Detect *inft-2(ok1296)* allele deletion
oDS321	ATTCAACGGTCGAACAGAGC	
oDS322	CCGTTTTCTTCTGCTTCCTG	
oDS399	CGGGGTACCGACGTCAGGCGGCCGCGGACCGGTAAAA**ATG**GTGAAGAAGCGCCAAAAC	Amplify *inft-2* cDNA
oDS400	TCATCTAGAA**TCA**AACTGGACTTCCTACCAAGG	
oDS416	ACGAAGATGAACTTGTCGGC	Detect *cyk-1(ok2300)* allele deletion
oDS417	CAATGCAATGATGGAAGTCG	
oDS418	ACCGCTCTCAGCTTGTCAAT	

Primers (cont'd)

Oligo	Sequence	Use
oDS430	TCGTCTGATGATGATGGAC	Sequence *inft-2* cDNA
oDS431	TCCAAGACCATCCAACGGAG	
oDS432	ACATCCACTTCTCCCGTTC	
oDS501	TGCAAGTTGTTTGGTACGGA	Detect *cdc-42(gk388)* allele deletion
oDS502	CAAGAATGGGGTCTTTGAGC	
oDS503	ACGGCGTAATTGTCGAAGAC	
oDS646	AATGCCAGTGGAGAAGGAGC	Detect *cyk-1(or596ts)* allele. Use with oDS417
oDS694	CGGGGTACCCCCGGGCATAAAA**ATG**GAAGAACTCACGAAAACAGTTCGG	Amplify *exc-5* cDNA
oDS695	TCAACTAGTA**TTA**TACCGGTGCAGCTCCTTCAGATTGCTCGGATCCAGAATTCCG	
oDS696	TCCAGATTTGAGAAGTTCGC	Sequence *exc-5* cDNA
oDS697	TTACAAGCAGCTGCACATGC	
oDS703	CGGGATATCGGTACCCATAAAA**ATG**TCTAGCGATGATTATGAGTCAATTG	Amplify *cyk-1b* cDNA
oDS704	TCAGCGGCCGC**TCA**TGCTGAGCGGAAATCATTAAGACGTGCGAGAAG	
oDS705	GAGAATCATTTGCCTTGTCAGG	Sequence *cyk-1b* cDNA
oDS706	CAGTTATTGGCGGTAGAGC	

Spinning Disk Microscopy Settings

- INFT-2::GFP (Fig. 2B) grown at 25°C. GFP (488nm) laser power at 10.4%, EM gain 595, and exposure 360ms. TagRFP (561nm) laser power at 5.5%, EM gain 570, and exposure 150ms.
- Venus::INFT-2 (Fig. 2C, D) grown at 22°C. CFP (445nm) laser power at 1.0%, EM gain 650, and exposure 400ms. YFP (514nm) laser power at 15.0%, EM gain 605, and exposure 700ms. TagRFP (561nm) laser power at 10.0%, EM gain 600, exposure 700ms.
- CYK-1::GFP (Fig. 2E) grown at 25°C. GFP (488nm) laser power at 10.0%, EM gain 521, and exposure 600ms. TagRFP (561nm) laser power at 5.0%, EM gain 570, and exposure 260ms.
- Venus::CYK-1 (Fig. 2F) grown at 25°C. CFP (445nm) laser power at 1.0%, EM gain 650, and exposure 400ms. YFP (514nm) laser power at 14.4%, EM gain 605, and exposure 700ms. TagRFP (561nm) laser power at 10.0%, EM gain 685, exposure 685ms.
- Venus::INFT-2 (Fig. 4C, D) in *wild-type* subjected to temperature shift (15°C to 25°C) as control. CFP (445nm) laser power at 1.0%, EM gain 260, and exposure 400ms. YFP (514nm) laser power at 10.0%, EM gain 600, and exposure 650ms. TagRFP (561nm) laser power at 10.0%, EM gain 590, exposure 320ms.
- Venus::INFT-2 (Fig. 4C, D) in *cyk-1(ts)* subjected to temperature shift (15°C to 25°C) to reduce CYK-1 function. CFP (445nm) laser power at 1.0%, EM gain 260, and exposure 350ms. YFP (514nm) laser power at 10.0%, EM gain 600, and exposure 650ms. TagRFP (561nm) laser power at 3.0%, EM gain 590, exposure 400ms.

Supplementary References

Andersen, E. C., Saffer, A. M. and Horvitz, H. R. (2008). Multiple levels of redundant processes inhibit *Caenorhabditis elegans* vulval cell fates. *Genetics* **179**, 2001-2012.

Brenner, S. (1974). The genetics of *Caenorhabditis elegans*. *Genetics* **77**, 71-94.

Chalkia, D., Nikolaidis, N., Makalowski, W., Klein, J. and Nei, M. (2008). Origins and evolution of the formin multigene family that is involved in the formation of actin filaments. *Mol Biol Evol* **25**, 2717-2733.

Edgley, M. L., Baillie, D. L., Riddle, D. L. and Rose, A. M. (2006). Genetic balancers. *WormBook*.

Evans, T. C. (2006). Transformation and Microinjection. *WormBook*.

Granato, M., Schnabel, H. and Schnabel, R. (1994). *pha-1*, a selectable marker for gene transfer in *C. elegans*. *Nucleic Acids Research* **22**, 1762-1763.

Johnston, R. J., Jr., Copeland, J. W., Fasnacht, M., Etchberger, J. F., Liu, J., Honig, B. and Hobert, O. (2006). An unusual Zn-finger/FH2 domain protein controls a left/right asymmetric neuronal fate decision in *C. elegans*. *Development* **133**, 3317-3328.

Liu, R., Linardopoulou, E. V., Osborn, G. E. and Parkhurst, S. M. (2010). Formins in development: orchestrating body plan origami. *Biochim. Biophys. Acta* **1803**, 207-225.

Mi-Mi, L., Votra, S., Kemphues, K., Bretscher, A. and Pruyne, D. (2012). Z-line formins promote contractile lattice growth and maintenance in striated muscles of *C. elegans*. *J Cell Biol* **198**, 87-102.

Nezami, A. G., Poy, F. and Eck, M. J. (2006). Structure of the autoinhibitory switch in formin mDia1. *Structure* **14**, 257-263.

Radman, I., Greiss, S. and Chin, J. W. (2013). Efficient and rapid *C. elegans* transgenesis by bombardment and hygromycin B selection. *PLoS One* **8**, e76019.

Shaye, D. D. and Greenwald, I. (2015). The Disease-Associated Formin INF2/EXC-6 Organizes Lumen and Cell Outgrowth during Tubulogenesis by Regulating F-Actin and Microtubule Cytoskeletons. *Dev Cell* **32**, 743-755.

Sun, H., Schlondorff, J. S., Brown, E. J., Higgs, H. N. and Pollak, M. R. (2011). Rho activation of mDia formins is modulated by an interaction with inverted formin 2 (INF2). *Proc Natl Acad Sci USA* **108**, 2933-2938.